

Article

Application of Green Polymeric Nanocomposites for Enhanced Oil Recovery by Spontaneous Imbibition from Carbonate Reservoirs

Yaser Ahmadi ^{1,*}, Mohamed Arselene Ayari ^{2,3,*}, Meysam Olfati ¹, Seyyed Hossein Hosseini ¹, Amith Khandakar ⁴, Behzad Vaferi ^{5,6} and Martin Olazar ⁷

¹ Chemical and Petroleum Engineering Department, Ilam University, Ilam 69315516, Iran

² Department of Civil and Architectural Engineering, Qatar University, Doha 2713, Qatar

³ Technology Innovation and Engineering Education Unit, Qatar University, Doha 2713, Qatar

⁴ Department of Electrical Engineering, Qatar University, Doha 2713, Qatar

⁵ Department of Chemical Engineering, Shiraz Branch, Islamic Azad University, Shiraz 7198774731, Iran

⁶ Department of Advanced Calculations, Chemical, Petroleum, and Polymer Engineering Research Center, Shiraz Branch, Islamic Azad University, Shiraz 7198774731, Iran

⁷ Department of Chemical Engineering, University of the Basque Country (UPV/EHU), P.O. Box 644-E48080 Bilbao, Spain; martin.olazar@ehu.eus

* Correspondence: yaser.ahmadi@ilam.ac.ir (Y.A.); arslana@qu.edu.qa (M.A.A.)

Abstract: This study experimentally investigates the effect of green polymeric nanoparticles on the interfacial tension (IFT) and wettability of carbonate reservoirs to effectively change the enhanced oil recovery (EOR) parameters. This experimental study compares the performance of xanthan/magnetite/SiO₂ nanocomposites (NC) and several green materials, i.e., eucalyptus plant nanocomposites (ENC) and walnut shell ones (WNC) on the oil recovery with performing series of spontaneous imbibition tests. Scanning electron microscopy (SEM), X-ray diffraction (XRD), energy-dispersive X-ray spectroscopy (EDAX), and BET (Brunauer, Emmett, and Teller) surface analysis tests are also applied to monitor the morphology and crystalline structure of NC, ENC, and WNC. Then, the IFT and contact angle (CA) were measured in the presence of these materials under various reservoir conditions and solvent salinities. It was found that both ENC and WNC nanocomposites decreased CA and IFT, but ENC performed better than WNC under different salinities, namely, seawater (SW), double diluted salted (2 SW), ten times diluted seawater (10 SW), formation water (FW), and distilled water (DIW), which were applied at 70 °C, 2000 psi, and 0.05 wt.% nanocomposites concentration. Based on better results, ENC nanofluid at salinity concentrations of 10 SW and 2 SW ENC were selected for the EOR of carbonate rocks under reservoir conditions. The contact angles of ENC nanocomposites at the salinities of 2 SW and 10 SW were 49 and 43.4°, respectively. Zeta potential values were −44.39 and −46.58 for 2 SW and 10 SW ENC nanofluids, which is evidence of the high stability of ENC nanocomposites. The imbibition results at 70 °C and 2000 psi with 0.05 wt.% ENC at 10 SW and 2 SW led to incremental oil recoveries of 64.13% and 60.12%, respectively, compared to NC, which was 46.16%.

Keywords: green nanocomposites; walnut; eucalyptus; salinity; wettability; polymer



Citation: Ahmadi, Y.; Ayari, M.A.; Olfati, M.; Hosseini, S.H.; Khandakar, A.; Vaferi, B.; Olazar, M. Application of Green Polymeric Nanocomposites for Enhanced Oil Recovery by Spontaneous Imbibition from Carbonate Reservoirs. *Polymers* **2023**, *15*, 3064. <https://doi.org/10.3390/polym15143064>

Academic Editors: Abu Sadat Muhammad Sayem, Haruna Musa Moda, Deepti Gupta and Parikshit Goswami

Received: 10 June 2023

Revised: 6 July 2023

Accepted: 12 July 2023

Published: 17 July 2023



Copyright: © 2023 by the authors. Licensee MDPI, Basel, Switzerland. This article is an open access article distributed under the terms and conditions of the Creative Commons Attribution (CC BY) license (<https://creativecommons.org/licenses/by/4.0/>).

1. Introduction

Due to the low level of oil production by standard methods, studies have been approached based on the use of alkaline [1,2], polymer [3,4], and surfactant [5,6] chemicals to improve oil recovery. Changing brine composition in the injected water is known as a cost-effective and efficient method, which can affect EOR scenarios [7]. One of the standard plans to intensify the oil recovery in all types of reservoirs is the injection of low concentrations of brine, known as low salinity flooding [8]. The main advantages of flooding with low salinity are its lower cost compared to expensive chemical methods and the fact

that no extra materials are required for flooding with low salinity [9]. Changing water composition in intense salinity flooding is a fascinating topic, and researchers have focused on it to maximize oil recovery [10,11]. Therefore, EOR methods with different water flooding methods have been recently used by changing water composition, that is, changing salinity or adding nanoparticles to the water to decrease residual oil saturation [8]. The small size and high specific surface area of nanoparticles are favorable characteristics to increase EOR through changes in the involved parameters [12–14], such as IFT [15] and CA. Studies dealing with changes in these parameters in the presence of novel nanoparticles are highly relevant. Furthermore, given their low concentration required, they are known as cost-effective materials with many applications in petroleum engineering [16,17].

Nanoparticles such as alumina [18,19], silica [20,21], nickel oxide [22], silver [23], and magnetite [24,25] have recently been used in different processes, including enhanced oil recovery. For example, silica nanoparticles have been used in the sandstone reservoir as they effectively change the main parameters in porous media, such as IFT and CA [26]. They used Cedr extraction and silica nanoparticles by obtaining 5 wt.% as the CMC point for surfactant, and it was found that, as silica nanoparticles concentrations were increased from 0 to 2500 ppm, IFT was decreased from a base point of 15.5 to 13 mN/m. Moreover, it was seen that, due to increasing surfactant concentration from 0 to 10 wt.%, IFT decreased 35 to 11.9 mN/m. Maleki et al. (2023) used a combination of silica/alumina nanocomposites based on polyacrylamide for EOR to obtain reservoir parameters, such as IFT. It was found that IFT reduction was the most important parameter which control nanocomposite behavior. Based on the results, at different salinity of 250,000 ppm to 180,000 ppm, oil recovery of 95.83 and 70.33% were obtained [27]. Xanthan is another essential and environmentally friendly biopolymer with many applications in the oil industry. Fu et al. (2022) showed that xanthan efficiently increases ultimate recovery due to salt resistance properties, rheological properties, great thickening, and improvement in viscosity [28]. Modified Xanthan in their study increased EOR 7% more than base Xanthan due to increasing viscosity up to three times. Nanoparticles produce positive changes in the porous environment, and they can easily travel through low-porosity media; salinity is an essential factor that must be studied in detail [29]. Navaie et al. (2022) used Xanthan gum as a natural surfactant for EOR [30]. It was concluded that the contact angle was decreased from 60.52 to 16.71° in the carbonate reservoir and 50.1 to 8.87° in the sandstone reservoirs. Moreover, it was observed that oil recovery was increased by up to 28.6%, and IFT was decreased by up to 74% in the presence of solution. Ali et al. (2019) used a combination of silica and xanthan (ZnO/SiO₂/xanthan) nanocomposites to modify the main parameters involving EOR (IFT and CA), and based on their results, the above two parameters are significantly improved in the presence of nanocomposites [20]. Based on their results, at 2000 ppm, IFT decreased from 31.8 to 2.016 mN/m, and the recovery factor increased from 46.96% to 66.24%. Motraghi et al. (2023) used silica/KCl/Xanthan to check IFT behavior [31]. Different solvent concentrations of 5%, 10%, 15% and at 25, 50, and 75 °C, and it was found that 1000 ppm of nanocomposites at 75 °C were the optimum value for IFT reduction. The presence of ferrofluids, such as magnetite nanoparticles, could also influence the parameters involving EOR; that is, they reduce viscosity and shear stress. Aristizábal-Fontal et al. (2018) showed that viscosity and shear stress were decreased by up to 81% and 78%, respectively, in heavy oil [32]. Magnetite nanoparticles have wide applications in the oil industry, especially in problematic wells and conditions involving asphaltene precipitation. Betancur et al. (2016) reported that magnetite can adsorb asphaltene up to 61 mg/g, and decrease asphaltene aggregation by up to 39% [33]. Recently, the use of green nanomaterials has found high popularity as they are safe from the environment and human health perspectives [34,35]. Furthermore, principles of green chemistry help synthesize nanomaterials without toxic components [36] and save energy and renewable inputs [37]. Green technology also means using nanomaterials to make the current production procedures and their products in an environmentally friendly way. Recently, our team developed a new polymeric material of green nanocomposites (Xanthan/SiO₂/ZnO)

for EOR based on the main parameters of this process (IFT and CA) at different salinity conditions. It was observed that green nanocomposites have high efficiency for EOR from carbonate reservoirs at different salinity conditions. Thus, CA and IFT were reduced to significantly lower values than those corresponding to commercial silica, and oil recovery at 2 SW and 10 SW salinity conditions increased to 25.1% and 34.1%, respectively [38]. Ali et al. (2020) utilized magnetite/xanthan/silica for the wettability alteration and IFT reduction, with xanthan being synthesized from the *Alocasia macrorrhiza* plant. The application of 250 to 1500 ppm concentration of the materials results in wettability alteration from the strongly oil-wet to the water-wet in the carbonate reservoir, and IFT decreased in the presence of nanocomposites [24]. According to their results, IFT was decreased from 28.3 to 4.35 mN/m, and contact angle was decreased from 134 to 28° after using nanocomposites. As it was mentioned, the main effective parameters are IFT and CA reduction, and Table 1 summarized the last works for EOR in the presence of nanoparticles.

Table 1. IFT and CA change in the presence of nanoparticles.

NPs	IFT (mN/N) Clean/with NPs	Contact Angle (°) Clean/with NPs	Ref.
SiO ₂	38.5/1.45	134/82	[39]
Fe ₂ O ₃	38.5/2.75	132.5/101	[39]
SiO ₂	38.4/26.5	90/60	[40]
SiO ₂	-	135.5/66	[41]
SiO ₂	20/1.87	-	[42]
ZnO/SiO ₂ /Xanthan	-	79/75 (2 SW)	[8]
ZnO/SiO ₂ /Xanthan	-	78/74 (10 SW)	[8]
SiO ₂	37.5/22.1	-	[43]
SiO ₂	35/10.9	-	[26]

It should be noted that although many EOR studies have already been conducted, there are limited works covering recovery tests at reservoir conditions. Moreover, too high concentrations have been commonly used for low permeability carbonate, and the mentioned plant is not easily accessible, especially in our region. Therefore, more accessible and cost-effective materials (i.e., eucalyptus plant and the walnut shell) are selected in this study instead of the *Alocasia macrorrhiza* plant, and their performance is compared with the base material (silica/xanthan/magnetite). Accordingly, the main novelty of this work was using cost-effective polymeric nanocomposites at different salinity at reservoir conditions.

2. Materials and Method

2.1. Materials

The core sample and crude oil are provided by one of Iran's carbonate oil reservoirs. Core porosity, permeability, and oil density and viscosity were 14.90%, 10.45 mD, and 10.00 cP, respectively. It was tried to select two same plugs for performing imbibition tests in the presence of nanocomposites, as shown in Figure 1. Initial carbonate plug mass (gram), plug length (cm), diameter (cm), and saturated oil plus mass (gram) were 112.20, 4.80, 3.80, and 119.20, respectively.

Solvents, salts (NaCl, CaCl₂, MgCl₂, KCl), and other chemical compounds were supplied by Merck and Aldrich with a purity of 99.5%. Xanthan gum (98% purity) was supplied by Aldrich company, iron chloride (FeCl₃), and sodium metasilicate (Na₂SiO₃) with 98% purity by Merck company. The values of brine composition, pH, and density are shown in Tables 2 and 3, respectively, according to different salinities. Distilled water was used during dilution. After the preparation of specific amounts of salts (FW, SW, 2 SW, and 10 SW), the solution was prepared with DIW, and it was homogenized before applying.

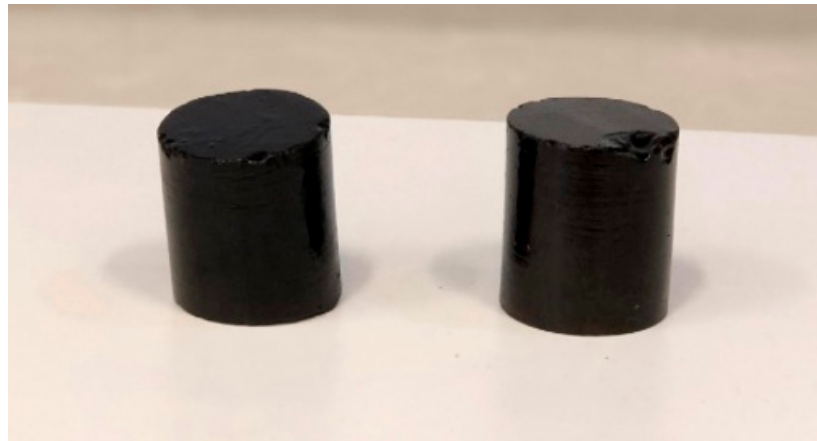


Figure 1. Plugs for performing imbibition tests.

Table 2. Brine composition.

Type	Ten Dilute SW (ppm)	Two Dilute SW (ppm)	SW (ppm)	Formation Water (ppm)
NaCl	2840	14,200	28,400	140,316
CaCl ₂	138	690	1380	40,287
MgCl ₂	643	3215	6430	2856
KCl	80	400	800	800

Table 3. pH and density of the brine.

Salinity Type	Density (g/mL)	pH (-)
DIW	1.00	7.00
SW	1.05	6.46
2 SW	1.01	6.93
10 SW	1.00	6.42
FW	1.07	8.11

2.2. Synthesizing Green Polymeric Nanocomposites (NC, WNC, and ENC)

The based material was xanthan/magnetite/SiO₂, and it was obtained based on Ali. et al., 2020 [24]. At the same condition, the desired plant extracts (from walnut bark or eucalyptus leaves) were prepared by heating 50 g of the sample (walnut bark powder or dried eucalyptus leaves) in 400 cm³ of distilled water at 80 °C for 40 min. Then, the samples obtained from both extracts were filtered, 2 g of FeCl₃ and 5 g of Na₂SiO₃ were added to 100 mL of the liquid solution at 80 °C, and the mixture was stirred at a pH value of 10 by adding NaOH. The stirring stops just after the formation of a black precipitate, and the solution filters for separation. The possible impurities are removed by heating the obtained residue at 400 °C and washing it with hot distilled water. Finally, the nanocomposites are synthesized by mixing 15 g of xanthan gum, 200 cm³ of ethanol, and the collected sediment under reflux conditions for 8 h at 80 °C. Figures 2a and 1b show details about the preparation of WNC and ENC nanocomposites.

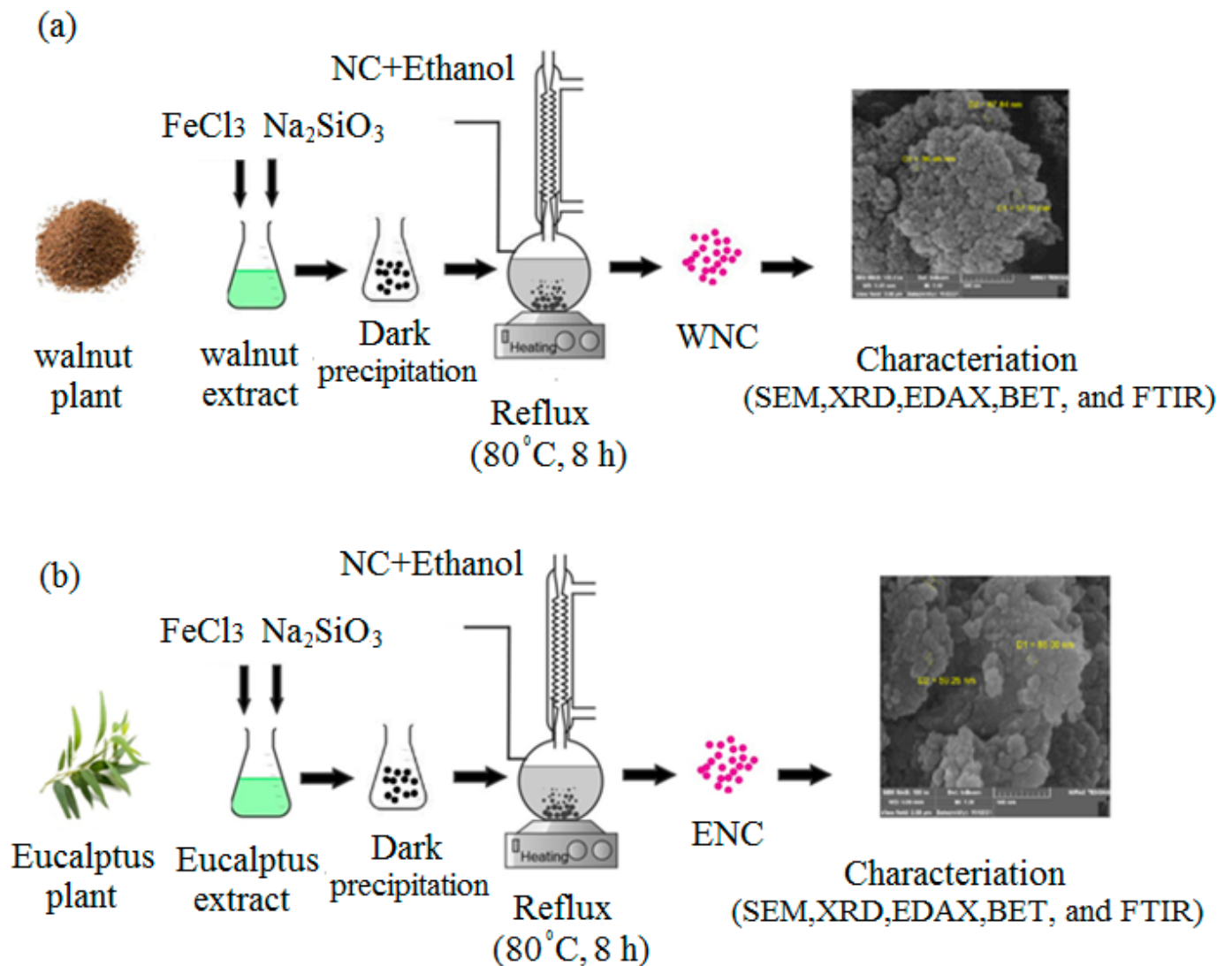
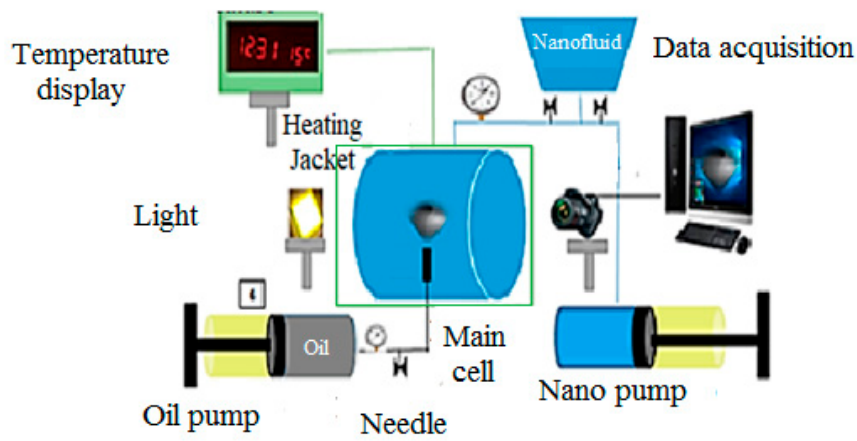


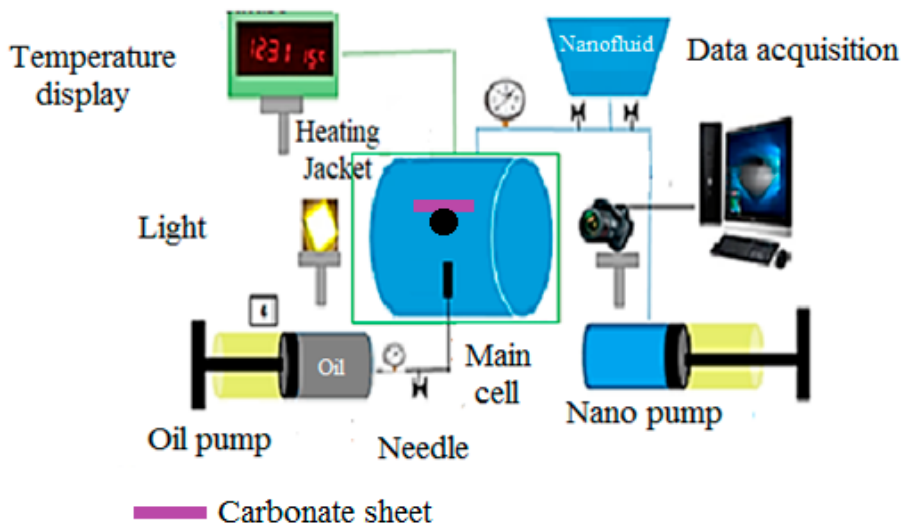
Figure 2. Details about the preparation of (a) Walnut and (b) Eucalyptus nanocomposites.

2.3. CA, IFT, and Imbibition Tests

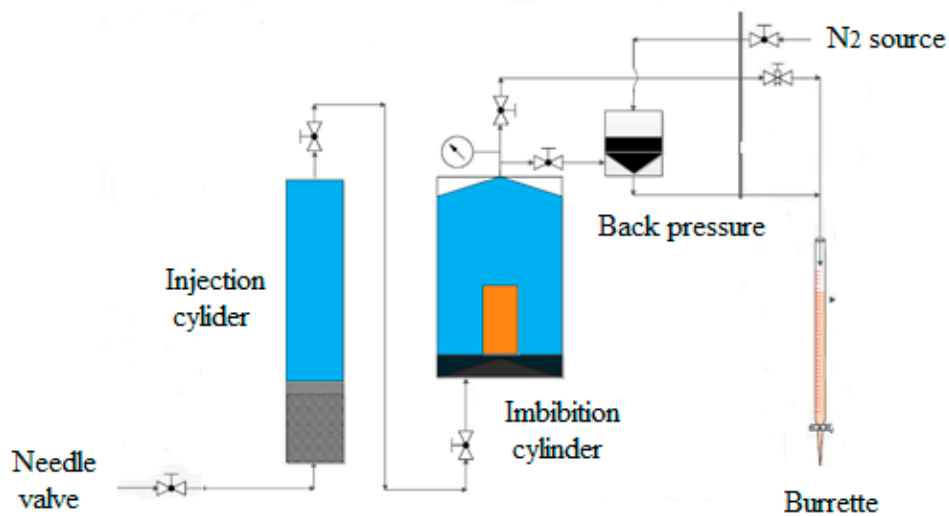
A schematic view of the equipment for IFT and CA tests is shown in Figures 3a and 2b, respectively, with the Petro AZMA model. After preparing the nanofluids at different salinities, they were transferred to the primary cell. Next, the crude oil was injected with an oil pump, and the drops were recorded with a camera. The system pressure was set to 2000 psi with a nano pump, and the temperature was 70°C in all tests. Finally, drops were calculated based on their analysis and IFT software. Instructions were rigorously followed for CA tests, and they differed only in the droplets on the carbonate sheets [38]. Figure 3c shows a schematic view of the equipment for the imbibition test, which was used for ascertaining oil recovery. Nanofluids containing 0.05 wt.% ENCs were prepared at two different salinities of 2 SW and 10 SW for IFT and CA tests, and the fluid was transferred to the primary cell surrounding the saturated oil core. The core initial mass, oil sodden group, initial oil saturation, and oil volume were recorded in the imbibition tests. Cell pressure and temperature were set at 70°C and 2000 psi, and runs were performed with 2 SW and 10 SW salinities. All experiments in our study were repeated three times, and their average values were reported.



(a)



(b)



(c)

Figure 3. Equipment for (a) IFT, (b) CA, and (c) Imbibition tests.

3. Results and Discussion

3.1. Chemical Composition and Surface Morphology of Nanocomposites

X-ray diffraction analysis was applied to observe the crystal structure with the PW1730 model. Figure 4 presents the X-ray diffraction spectrum of the base NC and those corresponding to WNCs and ENC. As observed, the XRD pattern of the sample without the extract is different from that containing the extract, which is evidence of the successful preparation of these compounds. The 2θ peaks at 11.32 and 27.82 correspond to eucalyptus plant and walnut shells, respectively [44–46].

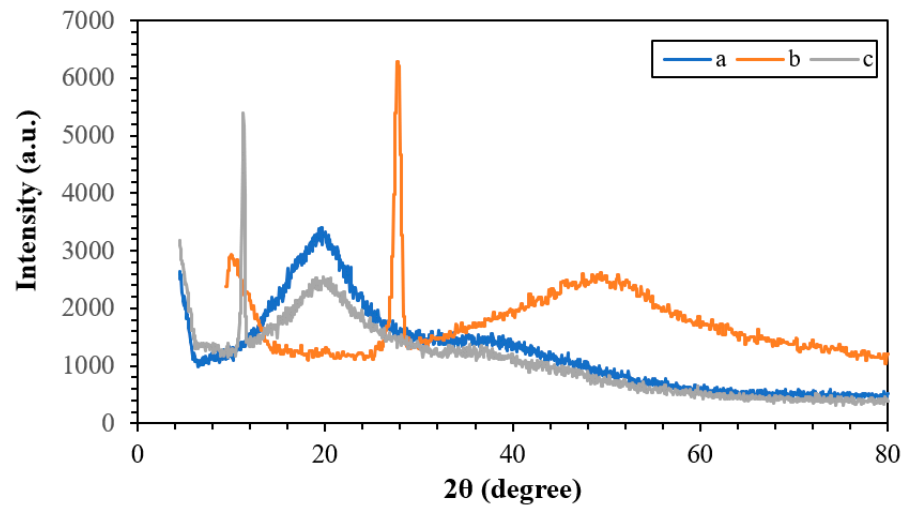


Figure 4. XRD spectrum of the (a) NC, (b) ENC, and (c) WNC.

Figure 5a–c introduce the scanning electron microscope images of NCs, ENCs, and WNCs, respectively. The morphological images show that the base NCs are spherical with a dimension range from 51 to 107 nm, and those modified with eucalyptus extract (ENCs) and walnut extract (WNCs) have average diameters of 59–86 nm and 36–67 nm, respectively.

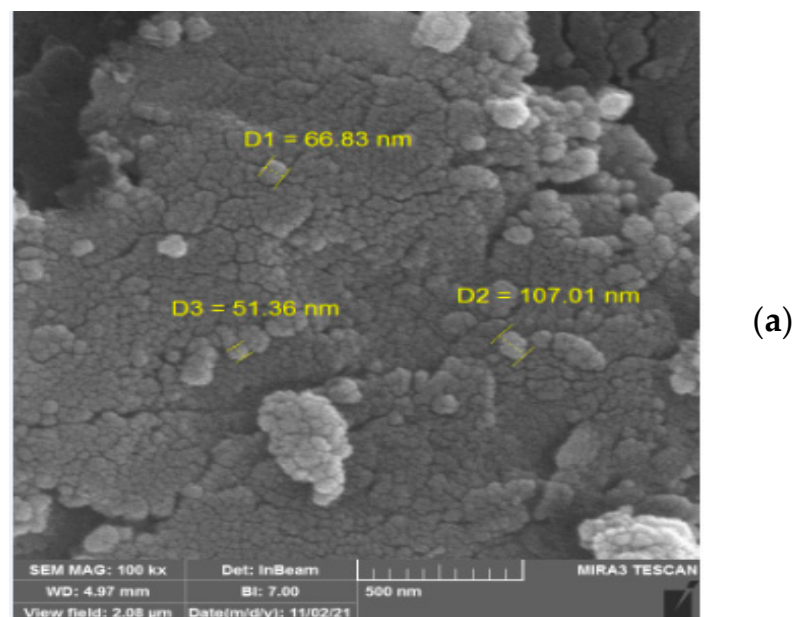


Figure 5. Cont.

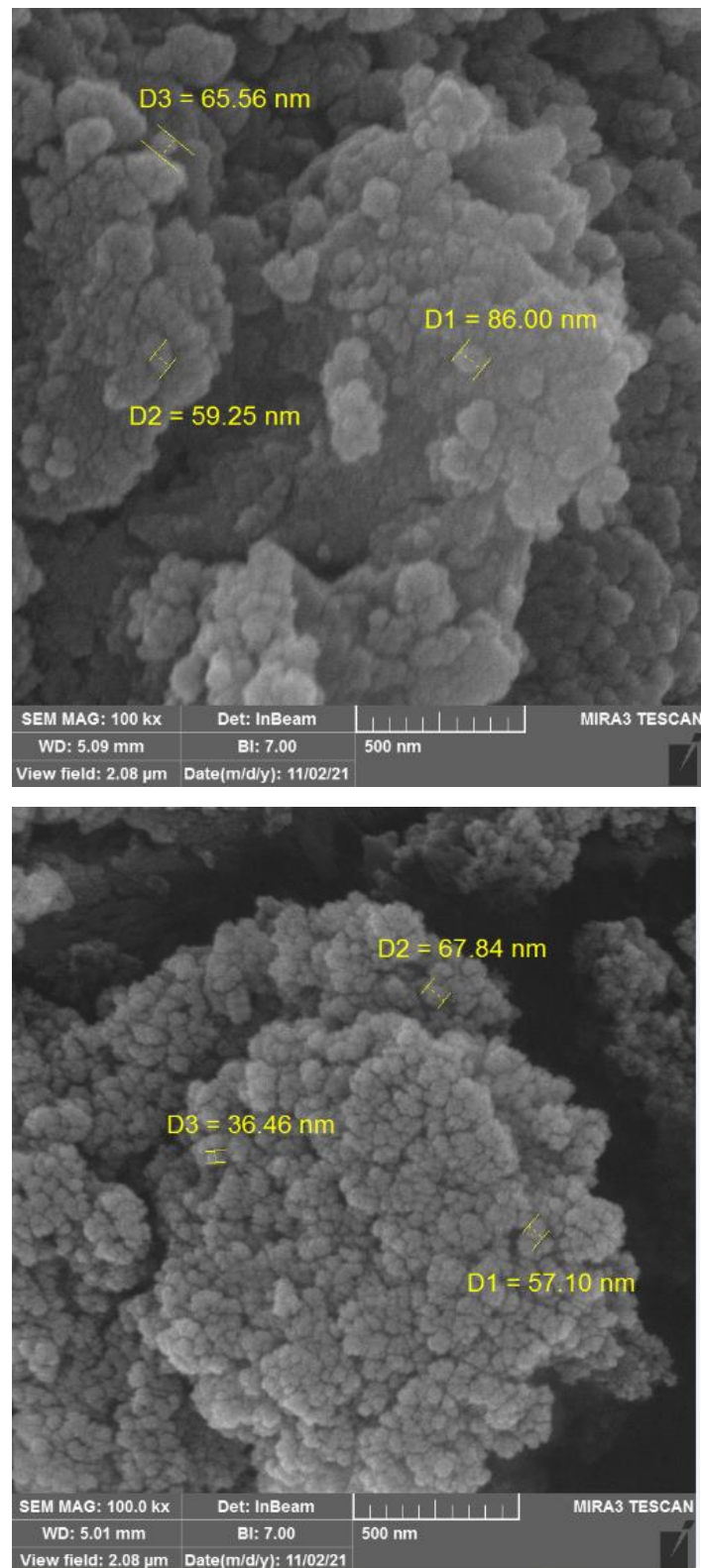


Figure 5. SEM images of (a) NC, (b) ENC, and (c) WNC.

Figure 6 depicts the FT-IR spectrum of NC, ENC, and WNC nanocomposites which were performed with the FTIR setup model Thermo AVATAR. Based on the results, the peaks that appeared at 3400 cm^{-1} are associated with O–H and N–H stretching vibrations, and those at 2925 , 1750 – 1650 , and 1420 cm^{-1} are related to C–H stretching vibrations,

C=O carbonyl groups, and C=C carbonyl groups, respectively. Furthermore, stretching vibrations related to C–O appeared at 1030 cm^{-1} .

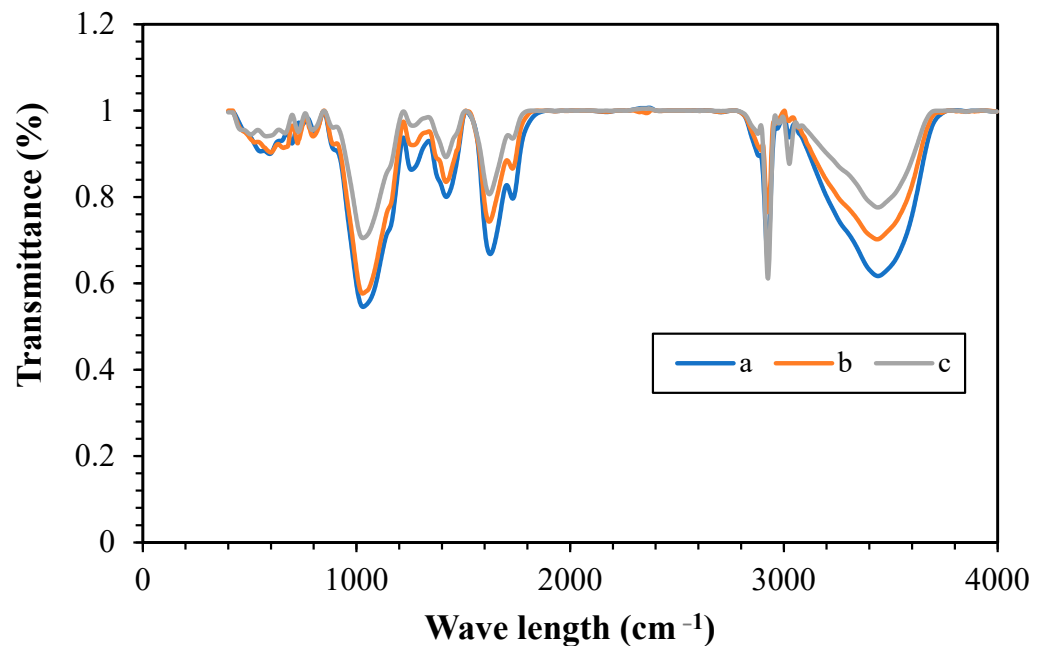


Figure 6. FT-IR spectrum of (a) NC, (b) ENC, and (c) WNC.

Energy Diffraction X-ray analyses (EDAX) were performed with the TESCAN MIRA2 model to investigate the elemental analysis of nanocomposites. EDAX tests for NC, ENC, and WNC nanocomposites are illustrated in Figure 7a, 7b, and 7c, respectively. Their elemental analysis is set out in Table 4. By examining the X-ray energy diffraction spectra, the presence of new elements corresponding to the plant extracts confirms that these nanoparticles have been correctly synthesized.

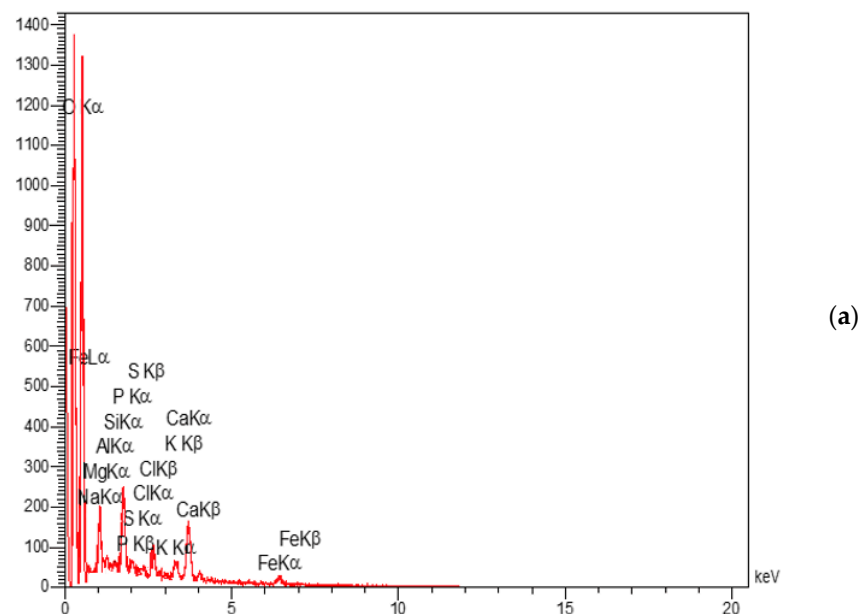


Figure 7. Cont.

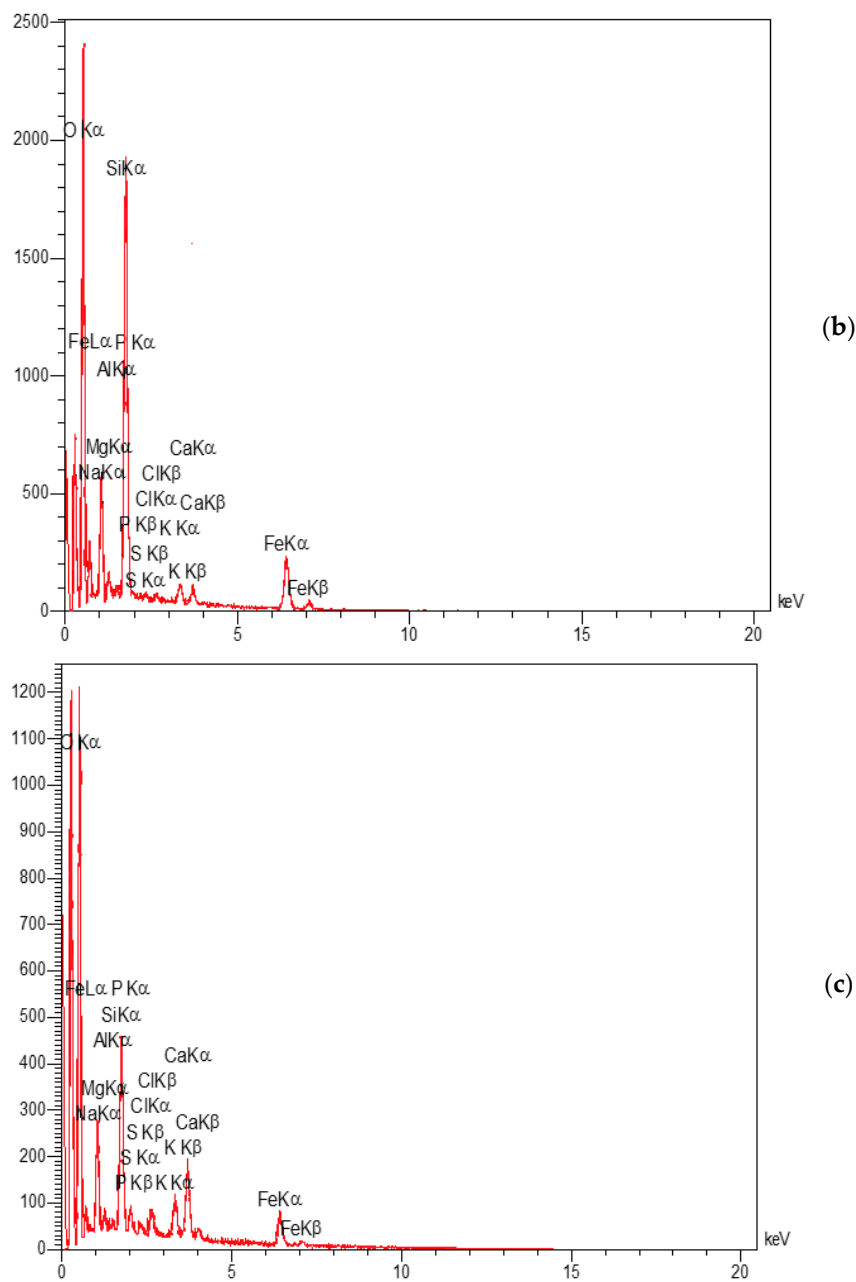


Figure 7. EDAX spectra of (a) NC, (b) ENC, and (c) WNC.

Table 4. EDAX elemental analysis of the nanocomposites.

Elements	NC (%)	ENC (%)	WNC (%)
C	44.78	29.78	43.57
O	47.17	47.63	43.41
Na	1.66	3.92	2.46
Mg	0.30	0.56	0.31
Al	0.17	0.24	0.15
Si	1.37	8.8	2.71
P	0.26	0.19	0.36
S	0.24	0.26	0.27
Cl	0.78	0.28	0.57
K	0.60	0.82	1.31
Ca	1.93	0.65	2.21
Fe	0.74	6.87	2.85

Figure 8 shows the isotherms of the N_2 adsorption–desorption of NC, ENC, and WNC samples determined based on the BET (Brunauer–Emmett–Teller) method with the BELSORP MINI II model. Table 5 reports the pore volume, average pore diameter, and BET surface area. The specific surface areas of NC, ENC, and WNC samples were 14.22, 36.04, and 30.97 m^2/g , respectively. Adding eucalyptus (ENCs) and walnut shells (WNCs) increased the pore volume of the nanocomposites, as well as their specific surface area.

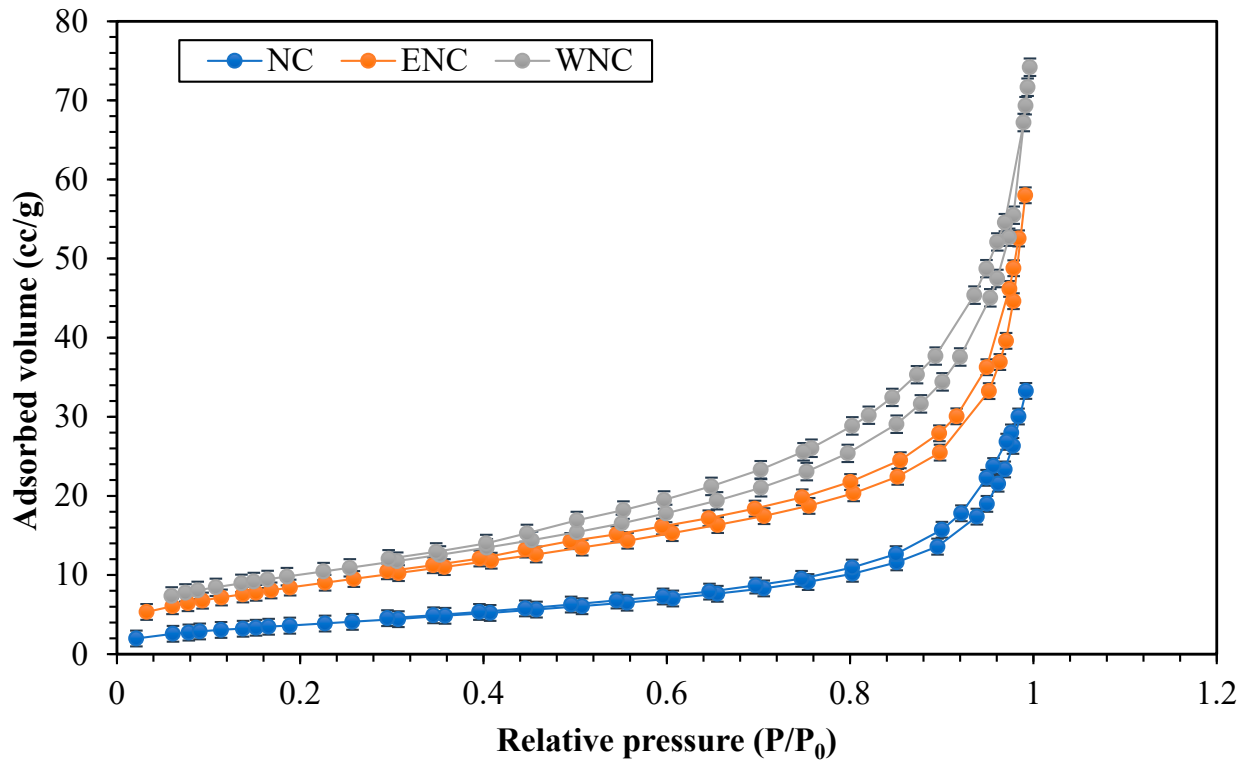


Figure 8. N_2 adsorption–desorption isotherms of NC, ENC, and WNC samples.

Table 5. Textural characteristics of the investigated nanocomposites.

Sample	Surface Area (m^2/g)	Average Pore Diameter (nm)	Pore Volume (cm^3 (STP)/g)
NC	14.22	14.29	0.05
ENC	36.04	11.65	0.10
WNC	30.97	11.35	0.08

3.2. Results of the IFT, CA, and Imbibition Tests

One of the crucial parameters to monitor when flooding with low salinity is the interfacial tension. Figure 9 shows the IFT between crude oil and water containing different nanocomposites (NC, ENC, and WNC) at 0.05 wt.% concentration under reservoir conditions (70 °C and 2000 psi). The results show that the interfacial tension decreases when salt water concentration is decreased among SW, 2 SW, and 10 SW, FW had the lowest IFT, and DIW had the highest IFT.

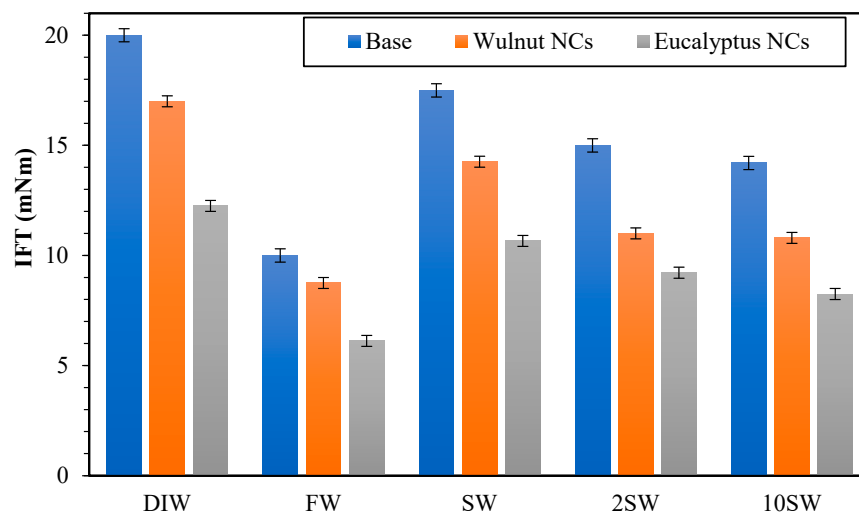


Figure 9. IFT of NC, WNC, and ENC.

Furthermore, interfacial tension with formation water is surprisingly lower than with the other salty solutions tested. Thus, when the salt water concentration was decreased, the surface-active material particles moved toward the contact surface, and the IFT decreased. As the concentration of saltwater was increased, the surface energy of the particles attenuated in the oil.

Among SW, 2 SW, and 10 SW, it was found that a solution of lower concentration reduces the solution ionic strength and, therefore, the interfacial tension, which enhances oil extraction [47]. This observation is quite consistent with the results reported by Nowrouzi et al. [48] and Ali et al. [49]. They described the effect of concentration and ionic compound of the seawater and reported that diluting the seawater can effectively reduce the IFT.

As observed in this figure, the IFT values of Magnetite/SiO₂/Xanthan nanocomposites decrease as the salinity of the solution is decreased. The main fact for IFT reduction lies in the use of xanthan gum in the structure of nanocomposites and the subsequent increase in tensile strength [38,50]. It should be noted that the data of IFT shown in Figure 9 correspond to the average of three replicates.

In addition, wettability is another crucial factor of a porous medium. This factor plays a vital role in water displacement and EOR parameters. The rock wettability is possible to change from oil-wet to water-wet in the presence of nanoparticles. An adsorbed layer of nanomaterials on the rock surface affects the fluid/rock as well as fluid/fluid interactions. A wide range of factors, including rock surface characteristics, nanoparticles size/concentration, and the nanoparticles-rocks interaction, determine the type of deposited layer on the rock surface as well as the resulting wettability alteration. Figure 10 shows the contact angles measured in the presence of different nanocomposites (NCs, WNCs, and ENCs) and different salinity levels (DIW, FW, SW, 2 SW, and 10 SW). The results of the runs under the reservoir temperature and pressure (70 °C and 2000 psi) with 0.05 wt.% nanocomposites concentration showed that the injection of ENC and WNC nanocomposites solutions increases the hydrophilic strength of the carbonate rock more than the injection of the base NC nanocomposites. Deionized water has the highest CA changes among other tested points. FW, 2 SW, and 10 SW dilute seawater solutions recorded the lowest wettability in the presence of NC, WNC, and ENC nanocomposites at the concentration of 0.05 wt.% under the temperature and pressure of the reservoir (70 °C and 2000 psi). Furthermore, all the nanocomposite solutions enhance the hydrophilic properties of carbonate rock, but (independently of the salinity) ENC and WNC nanocomposites decreased the CA more than the base NC nanocomposites. Based on these results, the green particle of the highest efficiency was chosen for further studies in the porous media. Thus, the ENC nanocomposites at the salinities of 2 SW and 10 SW were selected for performing imbibition

tests. The contact angles of ENC nanocomposites at the salinities of 2 SW and 10 SW were 49 and 43.4°, respectively.

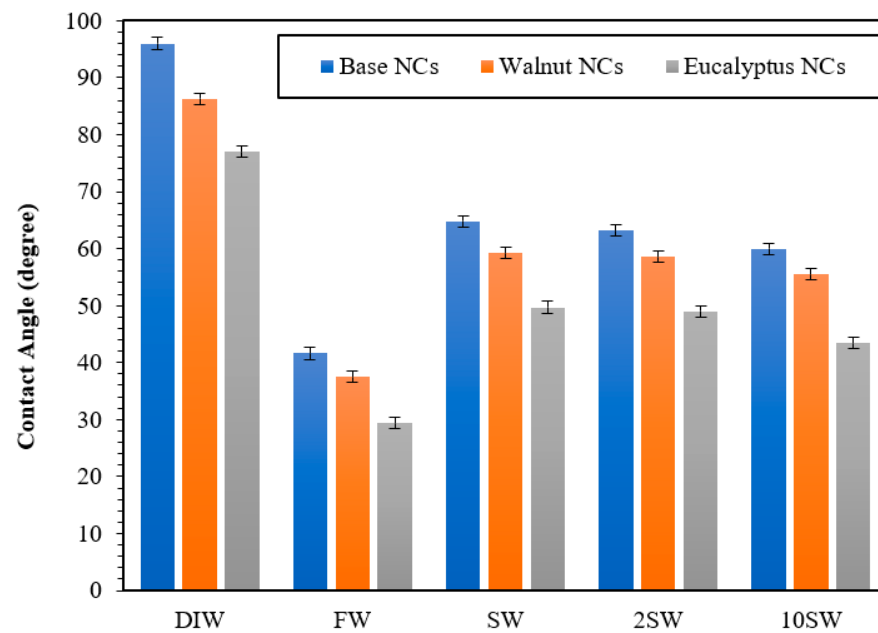


Figure 10. Contact angles for base NC, WNCs, and ENC at different salinities.

Figure 11 shows oil recovery test scenarios using base (NC) and ENC at different salinity of 2 SW and 10 SW under 2000 psi and 70 °C by using spontaneous imbibition tests. Oil recovery for the base, 2 SW, and 10 SW were 46.16, 60.12, and 64.13%, respectively. The changes in CA and IFT are responsible for increasing oil recovery with the nanocomposites. Furthermore, a highly relevant fact that must also be considered is stability. Thus, nanoparticle stability is one of the crucial factors that must be considered during flooding, especially in carbonate reservoirs of low permeability. Zeta potential was measured to ascertain stability in the presence of ENC nanocomposites with Malvern Zetasizer Nano ZS ZEN3600, Malvern Instruments Ltd, Malvern, United Kingdom and values of -44.39 and -46.58 were obtained for 2 SW and 10 SW, respectively. This finding clarifies that this nanocomposite is highly stable in the two solutions [51].

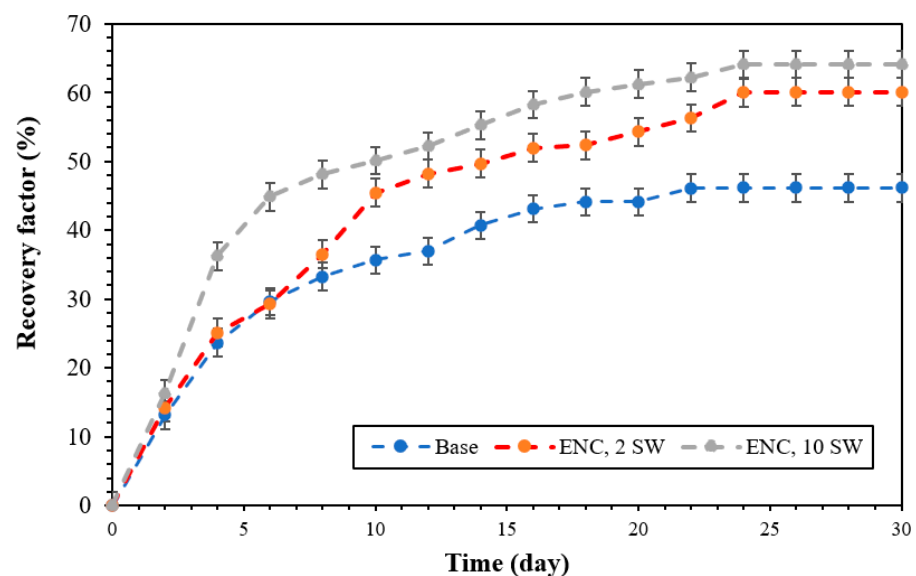


Figure 11. Oil recovery factors for base nanocomposites and ENC.

Table 6 compares the results of the current study with relevant previous works. Based on the results, nanocomposites had better tertiary oil recovery compared to others.

Table 6. Compare tertiary oil recovery with several relevant nanoparticles.

Nanoparticles	Permeability (mD)	Tertiary Oil Recovery (%)	References
ENC at 10 SW	10.45	17.97	Current study
SiO ₂	5.00	16.00	[52]
SiO ₂	0.21	16.00	[53]
SiO ₂ /Xanthan	2700	13.18	[54]
KCl/SiO ₂ /Xanthan	7.3	17.05	[55]

4. Conclusions

In this study, green polymeric nanocomposites of eucalyptus and walnut shell (ENC and WNC) were prepared at different salinity concentrations [DIW, FW, SW, 2 SW, and 10 SW] to enhance oil recovery under reservoir conditions [70 °C and 2000 psi] by spontaneous imbibition tests. The main advantages of this study were using cost-effective green materials at reservoir conditions at a low concentration of 0.05 wt.%. Based on the results of IFT and CA tests, ENC nanocomposites perform better than WNC nanocomposites, and they were selected for actual imbibition tests at 2 SW and 10 SW salinities (they are the most efficient solutions). In the presence of ENC nanocomposites, the zeta potential for 2 SW and 10 SW salinities are −44.39 and −46.58, respectively, which is evidence of the excellent stability of eucalyptus nanocomposites. Furthermore, the wettability of the carbonate rock changes towards hydrophilicity for low concentrations of brine. Two scenarios, i.e., 2 SW and 10 SW, with these eucalyptus nanocomposites led to the best results in wettability tests. The oil recoveries with ENC at 2 SW and 10 SW were 60.12% and 64.13%, respectively, compared to NC, which was 46.16%. The explanation for this result lies in the reduction of IFT and CA and their high stability. Future research should be devoted to ascertaining the influence of the parameters analyzed in this study (solution salinity and reservoir pressure and temperature) when the process is scaled up.

Author Contributions: Y.A.: Writing—original draft, Conceptualization, Investigation, Project Administration, Validation, Visualization, M.A.A.: Resources, Writing—review and editing, M.O. (Meysam Olfati): Writing—original draft, Formal analysis, S.H.H.: Writing—review and editing, Methodology, Supervision, A.K., B.V. and M.O. (Martin Olazar): Writing—review and editing. All authors have read and agreed to the published version of the manuscript.

Funding: The publication of this article was funded by the Qatar National Library.

Institutional Review Board Statement: Not applicable.

Informed Consent Statement: Not applicable.

Data Availability Statement: The datasets used and/or analyzed in the current study are available from the corresponding author upon reasonable request.

Conflicts of Interest: The authors declare no conflict of interest.

References

- Li, J.; Wang, W.; Gu, Y. Dynamic interfacial tension phenomenon and wettability alteration of crude oil-rock-alkaline-surfactant solution systems. In Proceedings of the SPE Annual Technical Conference and Exhibition, Houston, TX, USA, 26–29 September 2004; pp. 1803–1811. [CrossRef]
- Khlaifat, A.L.; Dakhllallah, D.; Sufyan, F. A Critical Review of Alkaline Flooding: Mechanism, Hybrid Flooding Methods, Laboratory Work, Pilot Projects, and Field Applications. *Energies* **2022**, *15*, 3820. [CrossRef]
- Fang, Y.; Yang, E.; Guo, S.; Cui, C.; Zhou, C. Study on micro remaining oil distribution of polymer flooding in Class-II B oil layer of Daqing Oilfield. *Energy* **2022**, *254*, 124479. [CrossRef]

4. Zhong, H.; He, Y.; Yang, E.; Bi, Y.; Yang, T. Modeling of microflow during viscoelastic polymer flooding in heterogenous reservoirs of Daqing Oilfield. *J. Pet. Sci. Eng.* **2022**, *210*, 110091. [[CrossRef](#)]
5. Saxena, N.; Kumar, A.; Mandal, A. Adsorption analysis of natural anionic surfactant for enhanced oil recovery: The role of mineralogy, salinity, alkalinity and nanoparticles. *J. Pet. Sci. Eng.* **2019**, *173*, 1264–1283. [[CrossRef](#)]
6. Kesarwani, H.; Saxena, A.; Mandal, A.; Sharma, S. Anionic/nonionic surfactant mixture for enhanced oil recovery through the investigation of adsorption, interfacial, rheological, and rock wetting characteristics. *Energy Fuels* **2021**, *35*, 3065–3078. [[CrossRef](#)]
7. Ahmadi, Y.; Hassanbeygi, M.; Kharrat, R. The Effect of Temperature and Injection Rate during Water Flooding Using Carbonate Core Samples: An Experimental Approach. *Reserv. Eng. Iran. J. Oil Gas Sci. Technol.* **2016**, *5*, 18–24.
8. Ahmadi, Y.; Malekpour, M.; Kikhavani, T.; Bayati, B. The study of the spontaneous oil imbibition in the presence of new polymer-coated nanocomposites compatible with reservoir conditions. *Pet. Sci. Technol.* **2022**. [[CrossRef](#)]
9. Xu, Z.X.; Li, S.Y.; Li, B.F.; Chen, D.Q.; Liu, Z.Y.; Li, Z.M. A review of development methods and EOR technologies for carbonate reservoirs. *Pet. Sci.* **2020**, *17*, 990–1013. [[CrossRef](#)]
10. Rodriguez, E.; Roberts, M.R.; Yu, H.; Huh, C.; Bryant, S.L. Enhanced migration of surface-treated nanoparticles in sedimentary rocks. In Proceedings of the SPE Annual Technical Conference and Exhibition, New Orleans, LA, USA, 4–7 October 2009; Volume 4, pp. 2058–2078. [[CrossRef](#)]
11. Tabora, E.A.; Alvarado, V.; Franco, C.A.; Cortés, F.B. Rheological demonstration of alteration in the heavy crude oil fluid structure upon addition of nanoparticles. *Fuel* **2017**, *189*, 322–333. [[CrossRef](#)]
12. Jafarbeigi, E.; Ahmadi, Y.; Mansouri, M.; Ayatollahi, S. Experimental Core Flooding Investigation of New ZnO- γ -Al₂O₃ Nanocomposites for Enhanced Oil Recovery in Carbonate Reservoirs. *ACS Omega* **2022**, *7*, 39107–39121. [[CrossRef](#)]
13. Jafarbeigi, E.; Kamari, E.; Salimi, F.; Mohammadidoust, A. Experimental study of the effects of a novel nanoparticle on enhanced oil recovery in carbonate porous media. *J. Pet. Sci. Eng.* **2020**, *195*, 107602. [[CrossRef](#)]
14. Hassan, Y.M.; Guan, B.H.; Chuan, L.K.; Sikiru, S.; Hamza, M.F.; Halilu, A.; Adam, A.A.; Abdulkadir, B.A.; Ayub, S. Stability and viscosity of zinc oxide–silicon dioxide nanocomposite in synthetic seawater supported by surfactant for enhanced oil recovery. *Nano-Struct. Nano-Objects* **2022**, *31*, 100902. [[CrossRef](#)]
15. Jafarbeigi, E.; Salimi, F.; Kamari, E.; Mansouri, M. Effects of modified graphene oxide (GO) nanofluid on wettability and IFT changes: Experimental study for EOR applications. *Pet. Sci.* **2022**, *19*, 1779–1792. [[CrossRef](#)]
16. Jafarbeigi, E.; Mohammadidoust, A.; Ranjbar, B. A review on applications of nanoparticles in the enhanced oil recovery in carbonate reservoirs. *Pet. Sci. Technol.* **2022**, *40*, 1811–1828. [[CrossRef](#)]
17. Ahmadi, Y.; Mansouri, M. An experimental investigation of using Ni-doped ZnO–ZrO₂ nanoparticles as a new asphaltene deposition inhibitor in ultra low carbonate porous media. *Energy Sources Part A Recover. Util. Environ. Eff.* **2022**, *44*, 9429–9447. [[CrossRef](#)]
18. Izadi, N.; Nasernejad, B. Newly engineered alumina quantum dot-based nanofluid in enhanced oil recovery at reservoir conditions. *Sci. Rep.* **2022**, *12*, 9505. [[CrossRef](#)]
19. Esmaeili-Faraj, S.H.; Hassanzadeh, A.; Shakeriankhou, F.; Hosseini, S.; Vaferi, B. Diesel fuel desulfurization by alumina/polymer nanocomposite membrane: Experimental analysis and modeling by the response surface methodology. *Chem. Eng. Process. Process Intensif.* **2021**, *164*, 108396. [[CrossRef](#)]
20. Ali, J.A.; Kolo, K.; Khaksar Manshad, A.; Stephen, K.D. Low-Salinity Polymeric Nanofluid-Enhanced Oil Recovery Using Green Polymer-Coated ZnO/SiO₂ Nanocomposites in the Upper Qamchuqa Formation in Kurdistan Region, Iraq. *Energy Fuels* **2019**, *33*, 927–937. [[CrossRef](#)]
21. Tohidian, M.; Ghaffarian, S.R.; Nouri, M.; Jaafarnia, E.; Haghighi, A.H. Polyelectrolyte nanocomposite membranes using imidazole-functionalized nanosilica for fuel cell applications. *J. Macromol. Sci. Part B* **2015**, *54*, 17–31. [[CrossRef](#)]
22. Xue, B.; Yang, Q.; Xia, K.; Li, Z.; Chen, G.Y.; Zhang, D.; Zhou, X. An AuNPs/mesoporous NiO/nickel foam nanocomposite as a miniaturized electrode for heavy metal detection in groundwater. *Engineering* **2022**. [[CrossRef](#)]
23. Yu, H.; Zhu, J.; Qiao, R.; Zhao, N.; Zhao, M.; Kong, L. Facile Preparation and Controllable Absorption of a Composite Based on PMo12/Ag Nanoparticles: Photodegradation Activity and Mechanism. *ChemistrySelect* **2022**, *7*, e202103668. [[CrossRef](#)]
24. Ali, J.; Manshad, A.K.; Imani, I.; Sajadi, S.M.; Keshavarz, A. Greenly Synthesized Magnetite@SiO₂@Xanthan Nanocomposites and Its Application in Enhanced Oil Recovery: IFT Reduction and Wettability Alteration. *Arab. J. Sci. Eng.* **2020**, *45*, 7751–7761. [[CrossRef](#)]
25. Rind, I.K.; Tuzen, M.; Sari, A.; Lanjwani, M.F.; Memon, N.; Saleh, T.A. Synthesis of TiO₂ nanoparticles loaded on magnetite nanoparticles modified kaolinite clay (KC) and their efficiency for As (III) adsorption. *Chem. Eng. Res. Des.* **2023**, *191*, 523–536. [[CrossRef](#)]
26. Emadi, S.; Shadzadeh, S.R.; Manshad, A.K.; Rahimi, A.M.; Mohammadi, A.H. Effect of nano silica particles on Interfacial Tension (IFT) and mobility control of natural surfactant (Cedr Extraction) solution in enhanced oil recovery process with nano—Surfactant flooding. *J. Mol. Liq.* **2017**, *248*, 163–167. [[CrossRef](#)]
27. Maleki, A.; Sedaee, B.; Bahramian, A.; Gharechelou, S.; Sarlak, N.; Mehdizad, A.; reza Rasaei, M.; Dehghan, A. Effect of alumina and silica nanocomposite based on polyacrylamide on light and heavy oil recovery in presence of formation water using micromodel. *Petroleum* **2023**. [[CrossRef](#)]

28. Fu, X.; Qin, F.; Liu, T.; Zhang, X. Enhanced Oil Recovery Performance and Solution Properties of Hydrophobic Associative Xanthan Gum. *Energy Fuels* **2022**, *36*, 181–194. [[CrossRef](#)]
29. Fawaz, J.; Mittal, V. Synthesis of polymer nanocomposites: Review of various techniques. In *Synthesis Techniques for Polymer Nanocomposites*; Mittal, V., Ed.; Springer: Berlin/Heidelberg, Germany, 2014; pp. 1–30. [[CrossRef](#)]
30. Navaie, F.; Esmailnezhad, E.; Choi, H.J. Xanthan gum-added natural surfactant solution of Chuback: A green and clean technique for enhanced oil recovery. *J. Mol. Liq.* **2022**, *354*, 118909. [[CrossRef](#)]
31. Motraghi, F.; Manshad, A.K.; Akbari, M.; Ali, J.A.; Sajadi, S.M.; Iglauer, S.; Keshavarz, A. Interfacial tension reduction of hybrid crude-oil/mutual-solvent systems under the influence of water salinity, temperature and green SiO₂/KCl/Xanthan nanocomposites. *Fuel* **2023**, *340*, 127464. [[CrossRef](#)]
32. Aristizábal-Fontal, J.E.; Cortés, F.B.; Franco, C.A. Viscosity reduction of extra heavy crude oil by magnetite nanoparticle-based ferrofluids. *Adsorpt. Sci. Technol.* **2018**, *36*, 23–45. [[CrossRef](#)]
33. Betancur, S.; Franco, C.A.; Cortés, F.B. Magnetite-silica nanoparticles with a core-shell structure for inhibiting the formation damage caused by the precipitation/deposition of asphaltene. In *Asphaltenes: Fundamentals, Applications and Future Developments*; Nova Science Publishers, Inc.: New York, NY, USA, 2016; pp. 85–138.
34. Anwar, A.; Masri, A.; Rao, K.; Rajendran, K.; Khan, N.A.; Shah, M.R.; Siddiqui, R. Antimicrobial activities of green synthesized gums-stabilized nanoparticles loaded with flavonoids. *Sci. Rep.* **2019**, *9*, 3122. [[CrossRef](#)]
35. Selim, Y.A.; Azb, M.A.; Ragab, I.; HM Abd El-Azim, M. Green synthesis of zinc oxide nanoparticles using aqueous extract of *Deverra tortuosa* and their cytotoxic activities. *Sci. Rep.* **2020**, *10*, 3445. [[CrossRef](#)]
36. Duan, H.; Wang, D.; Li, Y. Green chemistry for nanoparticle synthesis. *Chem. Soc. Rev.* **2015**, *44*, 5778–5792. [[CrossRef](#)] [[PubMed](#)]
37. Quadrelli, E.A. 25 years of energy and green chemistry: Saving, storing, distributing and using energy responsibly. *Green Chem.* **2016**, *18*, 328–330. [[CrossRef](#)]
38. Ahmadi, Y.; Javadi, F.; Kikhavandi, T. Effect of different salinity on low permeability carbonate reservoir recovery using a new green polymeric nanocomposites. *Energy Sources Part A Recover. Util. Environ. Eff.* **2023**, *45*, 1091–1103. [[CrossRef](#)]
39. Wang, Z.; Xu, Y.; Khan, N.; Zhu, C.; Gao, Y. Effects of the Surfactant, Polymer, and Crude Oil Properties on the Formation and Stabilization of Oil-Based Foam Liquid Films: Insights from the Microscale. *J. Mol. Liq.* **2023**, *373*, 121194. [[CrossRef](#)]
40. Li, X.; Liu, Y.; Hao, J.; Wang, W. Study of almond shell characteristics. *Materials* **2018**, *11*, 1782. [[CrossRef](#)]
41. Liu, C.; Li, Y.; Hou, Y. Effects of alkalinity of ionic liquids on the structure of biomass in pretreatment process. *Wood Sci. Technol.* **2019**, *53*, 177–189. [[CrossRef](#)]
42. Scatolino, M.V.; Dias, M.C.; Silva, D.W.; Bufalino, L.; Martins, M.A.; Piccoli, R.H.; Tonoli, G.H.D.; Londero, A.A.; Neto, V.O.; Mendes, L.M. Tannin-stabilized silver nanoparticles and citric acid added associated to cellulose nanofibrils: Effect on film antimicrobial properties. *SN Appl. Sci.* **2019**, *1243*. [[CrossRef](#)]
43. Rashid, F. Experimental Investigation of the Effect of Nanoparticles and Polymer on Interfacial Tension between Oil and Water during Enhanced Oil Recovery (EOR). Ph.D. Thesis, University of Salford, Salford, UK, 2021.
44. Joonaki, E.; Ghanaatian, S. The application of nanofluids for enhanced oil recovery: Effects on interfacial tension and coreflooding process. *Pet. Sci. Technol.* **2014**, *32*, 2599–2607. [[CrossRef](#)]
45. Seid Mohammadi, M.; Moghadasi, J.; Naseri, S. An experimental investigation of wettability alteration in carbonate reservoir using γ -Al₂O₃ nanoparticles. *Iran. J. Oil Gas Sci. Technol.* **2014**, *3*, 18–26.
46. Nazari Moghaddam, R.; Bahramian, A.; Fakhroueian, Z.; Karimi, A.; Arya, S. Comparative study of using nanoparticles for enhanced oil recovery: Wettability alteration of carbonate rocks. *Energy Fuels* **2015**, *29*, 2111–2119. [[CrossRef](#)]
47. Bhattacharjee, S. DLS and zeta potential—What they are and what they are not? *J. Control. Release* **2016**, *235*, 337–351. [[CrossRef](#)] [[PubMed](#)]
48. Nowrouzi, I.; Manshad, A.K.; Mohammadi, A.H. Effects of dissolved binary ionic compounds and different densities of brine on interfacial tension (IFT), wettability alteration, and contact angle in smart water and carbonated smart water injection processes in carbonate oil reservoirs. *J. Mol. Liq.* **2018**, *254*, 83–92. [[CrossRef](#)]
49. Ali, J.A.; Kolo, K.; Manshad, A.K.; Stephen, K.D. Potential application of low-salinity polymeric-nanofluid in carbonate oil reservoirs: IFT reduction, wettability alteration, rheology and emulsification characteristics. *J. Mol. Liq.* **2019**, *284*, 735–747. [[CrossRef](#)]
50. Zargartalebi, M.; Barati, N.; Kharrat, R. Influences of hydrophilic and hydrophobic silica nanoparticles on anionic surfactant properties: Interfacial and adsorption behaviors. *J. Pet. Sci. Eng.* **2014**, *119*, 36–43. [[CrossRef](#)]
51. Azarshin, S.; Moghadasi, J.; Aboosadi, Z.A. Surface functionalization of silica nanoparticles to improve the performance of water flooding in oil wet reservoirs. *Energy Explor. Exploit.* **2017**, *35*, 685–697. [[CrossRef](#)]
52. Zhao, M.; Lv, W.; Li, Y.; Dai, C.; Wang, X.; Zhou, H.; Zou, C.; Gao, M.; Zhang, Y.; Wu, Y. Study on the synergy between silica nanoparticles and surfactants for enhanced oil recovery during spontaneous imbibition. *J. Mol. Liq.* **2018**, *261*, 373–378. [[CrossRef](#)]
53. Xu, D.; Bai, B.; Wu, H.; Hou, J.; Meng, Z.; Sun, R.; Li, Z.; Lu, Y.; Kang, W. Mechanisms of imbibition enhanced oil recovery in low permeability reservoirs: Effect of IFT reduction and wettability alteration. *Fuel* **2019**, *244*, 110–119. [[CrossRef](#)]

54. Buitrago-Rincon, D.L.; Sadtler, V.; Mercado, R.A.; Roques-Carmes, T.; Marchal, P.; Muñoz-Navarro, S.F.; Sandoval, M.; Pedraza-Avella, J.A.; Lemaitre, C. Silica Nanoparticles in Xanthan Gum Solutions: Oil Recovery Efficiency in Core Flooding Tests. *Nanomaterials* **2023**, *13*, 925. [[CrossRef](#)]
55. Ahmadi, A.; Manshad, A.K.; Ali, J.A.; Iglauer, S.; Sajadi, S.M.; Keshavarz, A.; Mohammadi, A.H. Insight into nano-chemical enhanced oil recovery from carbonate reservoirs using environmentally friendly nanomaterials. *ACS Omega* **2022**, *7*, 36165–36174. [[CrossRef](#)]

Disclaimer/Publisher's Note: The statements, opinions and data contained in all publications are solely those of the individual author(s) and contributor(s) and not of MDPI and/or the editor(s). MDPI and/or the editor(s) disclaim responsibility for any injury to people or property resulting from any ideas, methods, instructions or products referred to in the content.